Towards GaSb/GaAs Quantum-Ring Single-Photon LEDs: Recent Progress and Prospects

Gizem Acar*[a], Lucie Leguay[b], Samuel Jones[a], Peter Hodgson[a], Andrei Schliwa[b], Manus Hayne[a]
[a]Department of Physics, Lancaster University, Lancaster LA1 4YB, UK; [b]Institute of Solid-State Physics, Technical University of Berlin, Berlin 10623, Germany

ABSTRACT

Advances in single-photon sources have proved pivotal to the progress of quantum information processing and secure communication systems. This study addresses the imperative need for developing commercially viable, electrically-driven single-photon sources capable of operating at or above room temperature with rapid response times and emission in the telecom wavelength range of 1260 to 1675 nm. We introduce an innovative single-photon light-emitting diode (SPLED) design employing GaAs quantum dots (QDs) and self-assembled GaSb quantum rings (QRs). The core of our design is an electron filter layer composed of GaAs QDs embedded in $Al_xGa_{1-x}As$, engineered to inject (single) electrons into an ensemble of type-II GaSb QRs in GaAs, where they recombine with strongly confined holes producing (single) photons at a wavelength governed by an optical cavity created using distributed Bragg reflectors (DBRs). This concept removes the need to select individual QD emitters, rendering the device highly suitable for scalable production. Our research demonstrates a comprehensive theoretical and experimental analysis using nextnano++ simulations and fabricated prototype device characteristics. Quite remarkably, we find that the emission properties of the SPLED devices actually improves as operational temperature is increased from 20 °C to 80 °C, making them attractive as practical devices.

Keywords: single-photon sources, single-photon light-emitting diode (SPLED), GaAs quantum dots, GaSb quantum rings, molecular beam epitaxy, single-electron filter, light-emitting diode, emission properties.

1. INTRODUCTION

In the realm of quantum technology, single-photon emitters stand at the forefront of revolutionizing communication and computing. By harnessing the unique principles of quantum mechanics, these devices are not just a scientific advancement; they are the keystones of a future where secure communication and supercharged computational capabilities become the norm[1]. The commercial development of single-photon emitters encompasses significant challenges. These devices require rapid response times, extensive tunability to accommodate various quantum technologies, and operational feasibility at or above room temperature, presenting considerable engineering obstacles[2]. Crucially, aligning their emission wavelength within the telecom band (1260 to 1675 nm) is essential for integrating them into existing fibre optic networks, a critical step towards practical quantum communication technology[3,4]. Developing a highly efficient single-photon emitter that operates at ambient temperature, emits at specific wavelengths, and responds quickly requires innovative approaches and advanced materials research[5].

Self-assembled QDs provide a possible answer to these problems. These structures have unique quantum mechanical properties, such as quantized energy levels and the ability to confine electrons and holes, which makes them appropriate for single-photon emission. QDs have captured the curiosity of researchers interested in utilising them as single-photon emitters due to their unusual zero-dimensional properties[6]. Of particular interest here are type-II (hole-confining) GaSb QRs, grown using molecular beam epitaxy (MBE), which exhibit less strain from lattice mismatch and fewer defects than GaSb QDs[7]. This makes them an alternative candidate for a variety of applications including memory storage[8], solar cells[9], light-emitting devices[10,11] and telecoms-wavelengths, room-temperature single photon sources[2].

This research introduces GaSb/GaAs QR SPLEDs, a novel concept in single-photon emitter technology. It takes advantage of the benefits of QRs to overcome the constraints of existing single-photon emitters. By incorporating QR structures into a regular LED framework, this approach potentially provides a scalable, efficient, and adaptable platform for single-photon emission, readily capable of emission in the critical telecom wavelength region. The suggested SPLED architecture includes a unique single-electron filter layer made up of highly non-uniform GaAs QDs embedded in $Al_xGa_{1-x}As$[12].

On application of a suitable voltage, the largest GaAs QD in this layer[13,14] allows a single electron to be injected into the GaSb QR layer, causing them to release a single photon and achieve the desired single-photon production. Even individual QRs are capable of emitting over a wide range of wavelengths[15], so the device has DBRs at the top and bottom, which impose wavelength selectivity via an optical cavity. The concept is expected to support high-speed operation due to the inherent speed of resonant tunnelling. As a result, we have proposed an electrically-driven, QR-based, telecoms-wavelength single-photon source readily capable of low-cost volume production, establishing it as a promising contender for practical quantum communication applications.

2. RESEARCH METHODS

2.1. Theoretical Methods

All theoretical simulations were performed using the nextnano++ software developed by nextnano GmbH[16]; a Schrödinger-Poisson-current solver specifically designed for semiconductor calculations, capable of handling both 1D and 3D simulations of nanostructures. The simulations were performed using both the effective mass method for 1D simulations and the eight-band k·p model for 3D simulations. For the study of dipole transitions, the eight-band k·p Schrödinger equation was solved for the Γ-conduction band, as well as for the heavy hole (HH), light hole (LH), and split-off (SO) hole valence bands. Two electron states and six-hole states were simulated, and the inter-band and intra-band matrix elements, transition energies, and oscillator strengths were calculated. Coulomb interaction is not included in this study.

From a general point of view, the multi-band k·p model combines accuracy and computational efficiency, presenting the underlying physics of the modelled nanostructures with clarity. It faithfully addresses all important aspects such as confinement, strain, piezo- and pyroelectricity, band-coupling, and -splitting for any geometry or composition[17]. After comparing it to alternative approaches such as the atomistic empirical tight-binding method[18] or the empirical pseudopotential theory[19], the k·p method was chosen as the most optimum computational approach. Considering the large size of the system modelled here and the consequently large number of atoms needed to be simulated, the performance of atomistic models would have been sub-optimal. The simulations using the multi-band k·p model described here were effectively executed on a contemporary computer, with processing times of up to seven hours for the largest QR.

2.2. Device Fabrication

The proposed architecture of our SPLEDs involves an ensemble of GaSb QRs, which were produced using the Stranski-Krastanow method by MBE, and a distinctive single-electron filter layer composed of deliberately highly non-uniform GaAs quantum dots formed by droplet epitaxy and embedded within an $Al_xGa_{1-x}As$ matrix [Fig. 1(a)]. The strategic placement and distribution of these GaAs QDs are crucial, as they play a pivotal role in the injection of single electrons into the GaSb QR layer, and, hence, performance of the device. DBRs are also integrated as key components of the device architecture at the top and bottom of the device, forming an optical cavity that enhances the selectivity of the emission wavelength. The fabrication of QR-SPLED devices encompassed a series of steps to develop contact parts for devices with mesas measuring approximately 100 μm in diameter, but it is in essence a fabrication process for a micro-LED, i.e., dispenses with any need to select an individual QD by emission wavelength or position, making it highly suitable for volume production. The device structure and schematic of the fabricated device are shown in Fig. 1 (a) and (b).

A pivotal stage in this process is the creation of a window in the Si_3N_4 dielectric isolation layer, applied via plasma-enhanced chemical vapor deposition (PECVD), that covers the SPLED's surface. This layer is essential for the metallization process, for maintaining the performance and for extending the lifetime of the device. Following the PECVD application, reactive ion etching (RIE) was employed to etch the sample and carve out the window layer. Top and bottom contacts were formed using Au/Ni/Au and AuGe/Ni/Au metal stacks, respectively, followed by Ti/Au bond pads, all by thermal evaporation. One of the last steps of the fabrication is the mesa etching process was applied using inductively coupled plasma (ICP). This step both helps define the active region where the light is produced and isolate the devices on the wafer from each other. After mesa etching, a passivation process was meticulously carried out to avoid oxidation of the side walls by the Si_3N_4 layer. The device was subsequently annealed to produce a low-resistance ohmic interface, an essential step for enhancing the electrical performance of the SPLEDs. The final stage of device preparation involved cleaving and wire bonding for electroluminescence (EL) and current-voltage (IV) measurements.

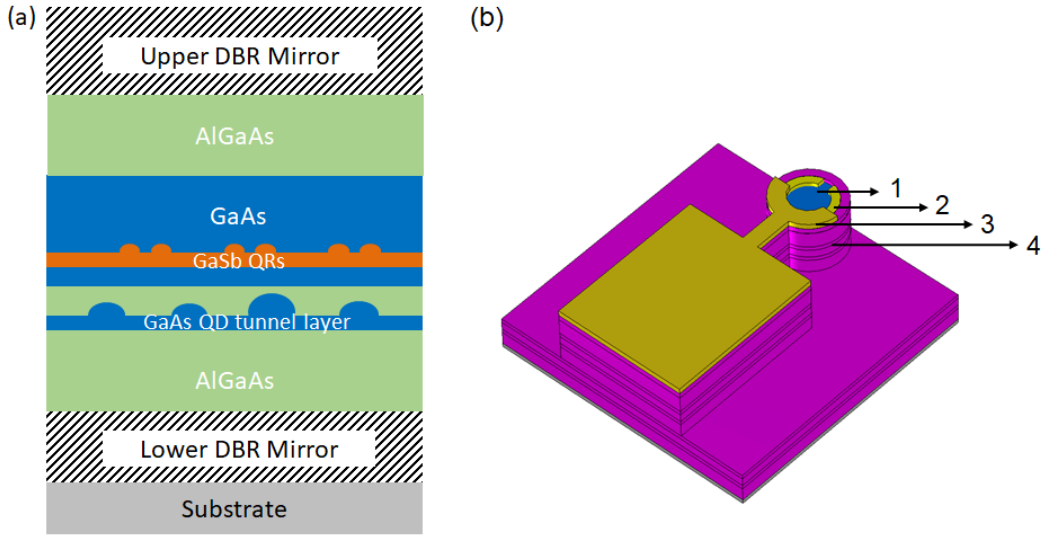

Fig. 1: Schematic of (a) the layer structure of the SPLED, and (b) the fabricated SPLED device, comprising (1) window layer fabrication, (2) contact metallisation, (3) bonding metallisation, and (4) mesa etching and passivation of side walls.

3. RESULTS AND DISCUSSION

3.1. Theoretical results

Complementary to the experimental investigation, a theoretical study was performed to achieve a general understanding of the system's electrical and optical properties. We first developed a one-dimensional (1D) model of the device including the n-doped region, the GaAs quantum dot (QD) surrounded by $Al_xGa_{1-x}As$, the GaSb quantum ring (QR) surrounded by GaAs and the p-doped region. The GaAs QD and GaSb QR were both represented by quantum wells in this 1D model. The GaSb QR region is the part of the device where electrons and holes recombine to emit light. The GaAs QD region represents an electron-filtering layer to inject a single electron, via tunnelling through the GaAs QD, towards the GaSb QR with the objective of building a single-photon LED. Fig. 2 shows the local band-edges of the 1D model. When no bias is applied [Fig. 2(a)], the Γ-band lies above the Fermi level which stands at 0 eV, thus indicating the absence of electrons in the GaAs QD. As an increasing bias is applied, the energy of Γ-band and the electron quasi-Fermi level both decrease until the latter lies above the Γ-band in the GaAs QD region at 1.5 V [Fig. 2(b)]. From this bias and above, electrons can tunnel through the GaAs QD electron-filtering layer, allowing them to be injected into the GaSb QR layer, where they can recombine with holes that are strongly confined within the GaSb QRs. Non-uniformity of GaAs QDs should allow passage of electrons through the largest GaAs QD at a threshold voltage[13], while a short pulse and/or Coulomb blockade could be used to ensure that just one electron is injected. This shows the potential of this design for the fabrication of a SPLED.

Next, we propose a three-dimensional (3D) model of a single GaSb QR surrounded by GaAs using the dimensions of the experimental structure obtained by TEM measurements [17]. The simulated QR has a height of 2 nm, an inner radius of 9 nm and an outer radius of 13 nm [see Fig. 3 (b)]. The local band-edges of the 3D model in the growth direction, z, are represented in Fig. 2(c), confirming the type-II band alignment of the structure. From there, we simulated other QRs with varying heights of 2.5 and 3 nm while keeping the same inner radius and outer radius as the first model to study the impact of the dimensions on the properties of the system. As expected, the energy of the conduction band decreases as the height of the QR increases while the energies of the valence bands increase. Fig. 2 (d) displays the emission spectra of the three QRs with the most probable inter-band dipole transitions, i.e., for a single electron-hole pair. As the height of the QR increases, the emission wavelength increases with a value of 1242 nm for the QR with a height of 2.5 nm. This coincidentally matches the main peak obtained in electroluminescence experiments, which is determined by the optical cavity formed between the DBRs. However, a capacitive charging energy, which is not included in our model, may need to be added to those calculated peaks[20]. For the first QR with a height of 2 nm, the most probable transition is between the two electron states E0 and E1 and the third- and fourth-hole states H2 and H3 while for the other two, the highest transition

energies are obtained between the electrons E0 and E1 and the first and second holes H0 and H1. For all three structures, the second emission peak corresponds to transitions between E0 and E1 and H4 and H5. We display the probability densities of the wavefunctions for one electron and three-hole states in Fig. 3 (b), and can easily categorize them according to their nodal planes: E0 is s-like while H0, H2 and H4 are p-like. It should be noted that due to the deep hole confining potential of the GaSb QRs they are highly likely to be occupied with more than one hole, which will blueshift the emission due to capacitive charging effects[15].

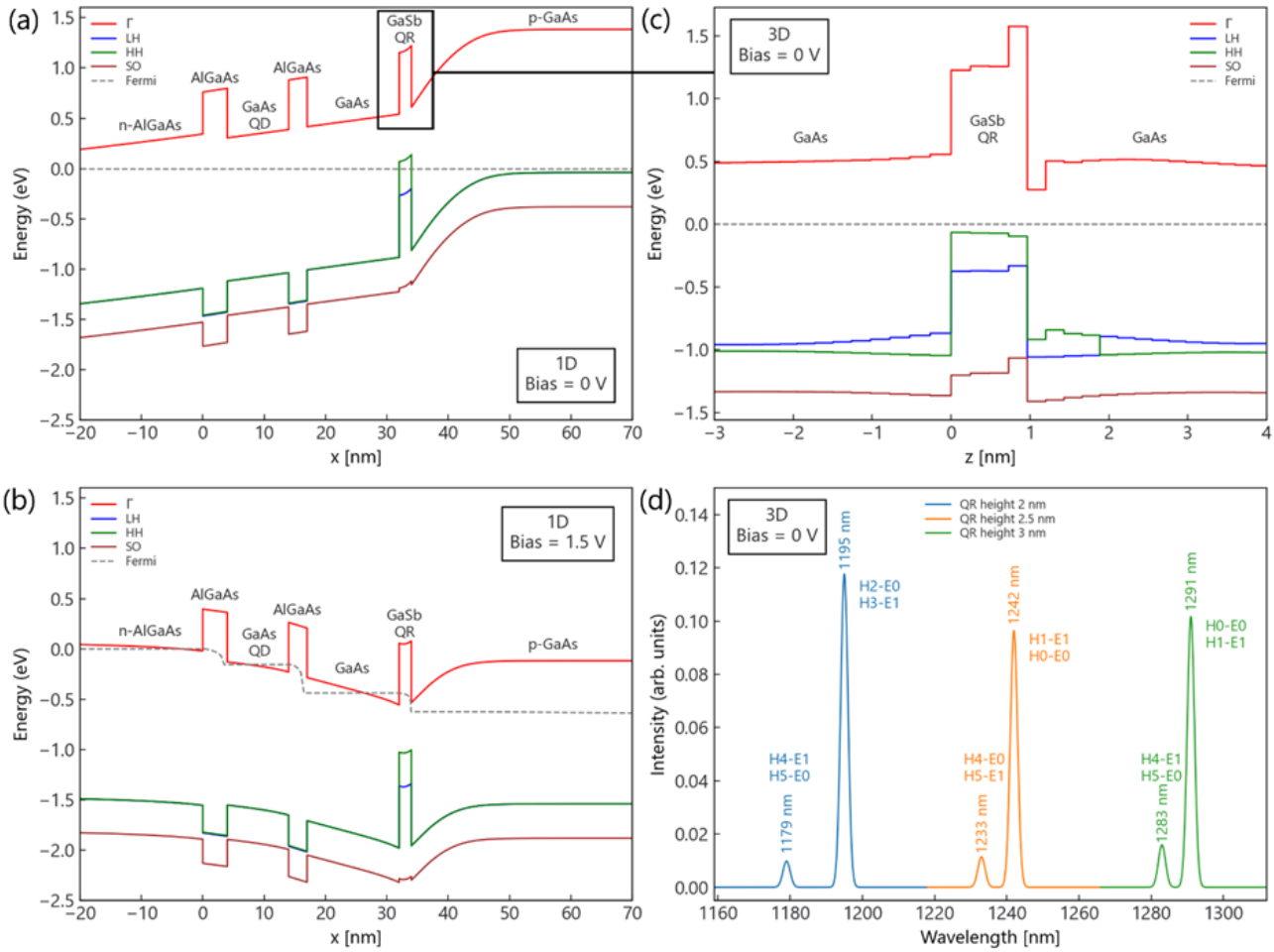

Fig. 2: Local band-edges of the 1D model calculated with strain, (a) without bias, and (b) with an applied bias of 1.5 V. (c) Local band-edges of the 3D QR model with a height of 2 nm, an inner radius of 9 nm and an outer radius of 13 nm in the direction of growth z, calculated with strain and without applied bias. (d) Calculated single-electron-hole-pair emission spectra for three different QR models with heights 2, 2.5 and 3 nm (and same inner radius 9 nm and outer radius 13 nm) with labels indicating the primary Γ-electron-hole transitions. It should be noted that due to the type-II nature of the QRs, capacitive charging with holes will blueshift the emission[15].

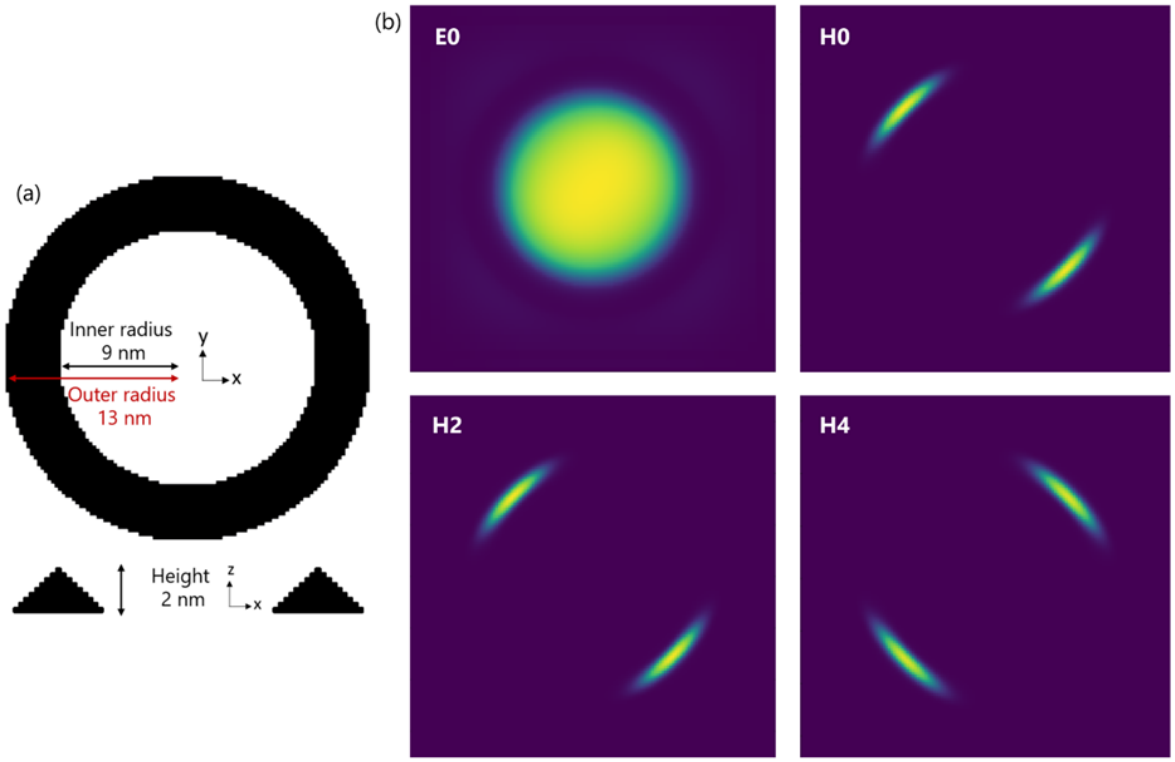

Fig. 3: (a) Description of the 3D QR model with relevant dimensions (height, inner radius, and outer radius). (b) Calculated electron and hole wavefunctions of the 3D QR model with a height of 2 nm, an inner radius of 9 nm, and an outer radius of 13 nm.

3.2. Experimental Results

Here, we present the results of electroluminescence (EL) studies of a GaSb QR-SPLED with a 100-µm mesa diameter, and an emission window with a diameter of 50 µm. The EL intensity-wavelength graph for the SPLED device demonstrates a strong and consistent emission across different current levels, as shown Fig. 4 (a), with a cavity peak at 1242 nm, just below the telecoms range. At either side of the cavity peak the normal LED (off-cavity resonance) emission is modulated by the transmission of the top DBR resulting in a series of peaks (sidebands). For these devices, the design wavelength of

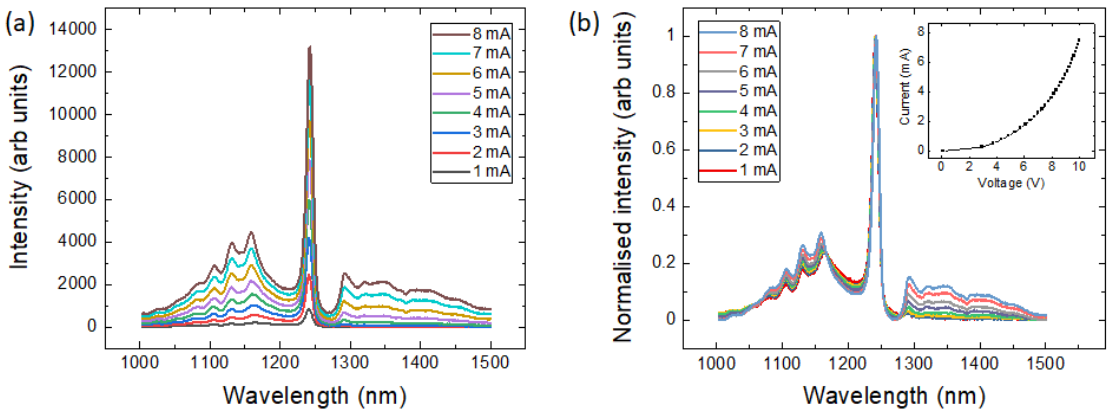

Fig. 4: (a) Electroluminescence intensity vs wavelength graph for different currents. (b) Normalised intensity vs wavelength graph for different currents and the current-voltage (IV) characteristics of the SPLED device (inset).

the cavity was matched to normal LED emission, but other devices have been fabricated with the cavity emission well into the telecoms band. When the intensity values at different currents were normalised, a notable reduction in the intensity of sidebands at lower currents was observed as shown in Fig. 4 (b). This indicates that the device exhibits improved performance when operating at these reduced current levels. The current-voltage (IV) characteristics of the SPLED device exhibit typical diode behaviour, resembling that of a conventional LED, as shown in the inset to Fig. 4 (b). The forward bias region shows an exponential increase in current with the applied voltage, a hallmark of diode-like behaviour and efficient charge carrier injection into the device.

To evaluate the device's performance above room temperature, which is advantageous for cooler-free operation, the devices were tested by elevating the temperature from 20 °C to 80 °C while maintaining a constant current as shown in Fig. 5. Increasing the temperature causes a small, but clearly discernible, redshift in the cavity emission peak wavelength, which is a well-known effect in vertical-cavity surface-emitting lasers that results from a change in the refractive index of the cavity, and not from a change in the semiconductor bandgap. The cavity peak wavelength is entirely determined by the optical properties of the cavity, and not by the semiconductor band structure. Much more interesting is the decrease in the background (off-resonance) normal LED emission, on both sides of the cavity peak, i.e., increasing the temperature reduces the emission at wavelengths other then the cavity. We speculate that this is the result of non-radiative recombination supressing the non-resonant emission but not the cavity emission, due to the enhanced recombination rate that the cavity imposes on the latter. Combined with the shift of the cavity peak to longer wavelengths, and the bandgap reduction which also redshifts the intrinsic emission profile of the QRs with increasing temperature, it would seem that, at least in these respects, operation of QR SPLEDs above room temperature may actually improve their emission, as well as being operationally advantageous in applications.

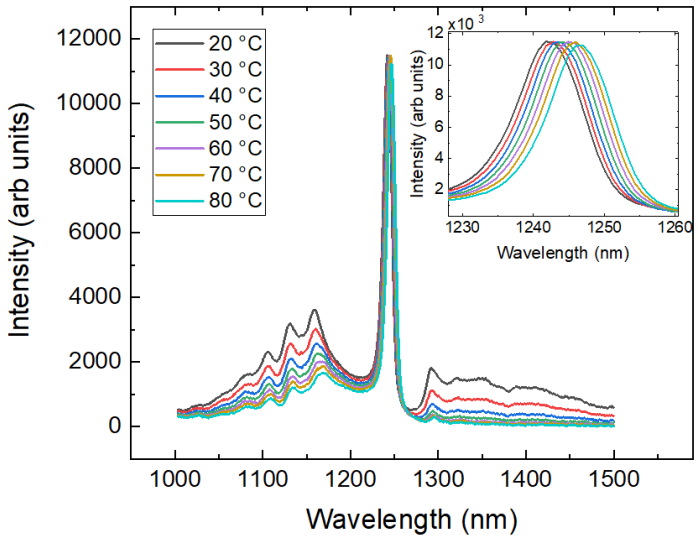

Fig. 5: Electroluminescence intensity vs wavelength from 20 °C to 80 °C under a condition of constant current. It can be seen that as temperature increases the intensity of the cavity peak increases relative to the non-resonant emission, which is highly advantageous for practical SPLED devices. The inset figure shows the magnified image of the shift in the cavity emission peak.

4. CONCLUSIONS

In this paper, we presented a theoretical study and analysis of the EL properties of the GaSb QR-SPLED, highlighting its potential for use in quantum communication technologies. In the theoretical study, we modelled the device in 1D and showed that, when a bias of ≥1.5 V is applied, electrons populate the GaAs QD region, allowing them to tunnel through into the GaSb layer, which is promising for the fabrication of a working SPLED with a single-electron filtering layer. We also simulated different GaSb QR systems in 3D and obtained emission wavelengths in the expected telecom range. We have established that SPLEDs exhibit robust and stable performance under various operational conditions, with excellent diode-like electrical behavior and consistent emission across different current levels. Notably, increasing operational

temperature from 20 °C up to 80 °C is observed to supress the non-resonant emission, while shifting the cavity peak (further) into the telecommunication band. These results quite remarkably imply that the GaSb QR SPLEDs may perhaps operate more effectively above rather than at room temperature.

ACKNOWLEDGMENTS

This work is supported by the European Union's Horizon 2020 research and innovation programme under the Marie Skłodowska-Curie grant agreement n° 956548, project Quantimony. Stefan Birner and Nextnano GmbH are also acknowledged for their support of the theoretical study.

REFERENCES

[1] C. Y. Lu *et al.* 2021 Quantum-dot single-photon sources for the quantum internet, Nature Nanotechnology, 16 12, 1294-1296.
[2] Young *et al*. Fine structure of strongly confined excitons in type-II GaSb quantum rings, AIP Advances 4, 117127 (2014).
[3] G. Moody *et al.* 2022 Roadmap on integrated quantum photonics, J. Phys. Photonics, 4 012501 (2022).
[4] X. Cao *et al*. Telecom wavelength single photon sources, J. Semicond.,40 071901 (2019).
[5] J. Lee *et al*. Integrated single photon emitters, AVS Quantum Science, 2.3 (2020).
[6] S. Buckley *et al.* Engineered quantum dot single-photon sources, Rep. Prog. Phys., 75 126503 (2012).
[7] R. Timm *et al.* Quantum ring formation and antimony segregation in GaSb⁄GaAs nanostructures, J. Vac. Sci. Technol. B 26, 1492-1503, (2008).
[8] T. Nowozin *et al.* Linking structural and electronic properties of high-purity self-assembled GaSb/GaAs quantum dots. Phys. Rev. B 86, 035305 (2012).
[9] P. J. Carrington *et al*. Enhanced infrared photo-response from GaSb/GaAs quantum ring solar cells, Appl. Phys. Lett., 101, 23, 231101 (2012).
[10] W.-H. Lin et al. Improved 1.3μm Electroluminescence of InGaAs-Capped Type-II GaSb/GaAs Quantum Rings at Room Temperature, IEEE Photonics Technol. Lett., 24, 14, 1203-1205 (2012).
[11] P. J. Carrington *et al.* Long-wavelength photoluminescence from stacked layers of high-quality type-II GaSb/GaAs quantum rings, Cryst. Growth Des., 13, 3, 1226-1230 (2013).
[12] M. Hayne *et al.* Single photon source. WO2018162894A1 (2018).
[13] L. Turyanska *et al.* Sharp-line electroluminescence from individual quantum dots by resonant tunnellingi njection of carriers, Appl. Phys. Lett. 89, 092106 (2006).
[14] M. J. Conterio *et al.* A quantum dot single photon source driven by resonant electrical injection, Appl. Phys. Lett. 103, 162108 (2013).
[15] P. D. Hodgson *et al.* GaSb quantum rings in GaAs/$Al_xGa_{1-x}As$ quantum wells, Journal of Applied Physics 119, 044305 (2016).
[16] S. Birner *et al.* nextnano: General Purpose 3-D Simulations. IEEE Trans. Electron Dev, 54 2137 (2007).
[17] A. Schliwa *et al.* Few-particle energies versus geometry and composition of $In_xGa_{1-x}As$/GaAs self-organized quantum dots. Phys. Rev. B **79**, 075443 (2009).
[18] A. Mittelstädt *et al.* Modeling electronic and optical properties of III–V quantum dots—selected recent developments. Light Sci. Appl. **11**, 1 (2022).
[19] L. W. Wang *et al.* Comparison of the k·p and direct diagonalization approaches to the electronic structure of InAs/GaAs quantum dots, Appl. Phys. Lett. 76, 339 (2000).
[20] R. J. Young *et al*. Optical observation of single-carrier charging in type-II quantum ring ensembles, Applied Physics Letters 100.8 (2012).